Marine Geology xxx (2009) xxx–xxx

Contents lists available at ScienceDirect

Marine Geology

journal homepage: www.elsevier.com/locate/margeo

Episodic methane concentrations at seep sites on the upper slope Opouawe Bank, southern Hikurangi Margin, New Zealand

A. Krabbenhoeft *, G.L. Netzeband [1,2], J. Bialas [3], C. Papenberg [4]

IFM-GEOMAR, Wischhofstraße 1-3, 24148 Kiel, Germany

ARTICLE INFO

Article history:
Received 13 July 2008
Received in revised form 15 July 2009
Accepted 6 August 2009
Available online xxxx

Keywords:
Methane
METS
seismics
seeps
vents
Hikurangi Margin
New Zealand

ABSTRACT

Along many active and some passive margins cold seeps are abundant and play an important role in the mechanisms of methane supply from the subsurface into seawater and atmosphere. With numerous cold seeps already known, the convergent Hikurangi Margin east of North Island, New Zealand, was selected as a target area for further detailed, multidisciplinary investigation of cold seeps within the New Vents and associated projects. Methane and temperature sensors (METS) were deployed at selected seep sites on the Opouawe Bank off the southeastern tip of North Island and near the southern end of the imbricate-thrust Hikurangi Margin, together with seismic ocean bottom stations. They remained in place for about 48 h while seismic data were collected. The seeps were associated with seep-related seismic structures. Methane concentrations were differing by an order of magnitude between neighbouring stations. The large differences at sites only 300 m apart, demonstrate that the seeps were small scale structures, and that plumes of discharged methane were very localised within the bottom water. High methane concentrations recorded at active seep sites at anticlinal structures indicate focused fluid flow. Methane discharge from the seafloor was episodic, which may result from enhanced fluid flow facilitated by reduced hydrostatic load at low tides. The strong semi-diurnal tidal currents also contribute to the fast dilution and mixing of the discharged methane in the seawater. Despite dispersal by currents, fluid flow through fissures, fractures, and faults close to the METS positions and tidal fluctuations are believed to explain most of the elevated methane concentrations registered by the METS. Small earthquakes do not appear to be correlated with seawater methane anomalies.

1. Introduction

The role of methane discharge in geological environments has become crucial in understanding changing climate (e.g. Kvenvolden, 1993). Intensive studies have been conducted, especially in marine continental margin environments where gas hydrates have the potential for huge methane discharge (e.g. Kvenvolden, 1988, 1998). Yet submarine methane discharge is imperfectly understood (Berndt, 2005).

Cold seeps are found along both active and passive continental margins. They are often associated with gas hydrate deposits (e.g. Suess et al., 1999; Bohrmann et al., 2003, Milkov, 2005). High methane concentrations have been observed in the bottom water in the proximity of active seep sites, with the methane concentrations decreasing rapidly with distance from the vent site as they become diluted by surrounding seawater (e.g. Faure et al., 2006, Mau et al., 2007).

Previous investigations of methane release on continental margins have generally involved measuring methane concentration in the water column by using methane sensors towed by a research vessel, or by vertical profiling using conductivity, temperature, and depth (CTD) casts (e.g. Faure et al., 2006, Mau et al., 2007). These measurements of methane concentration are “snapshots” in time, and problematical in that changes in methane concentrations can occur quickly in response to rapid dissolution or forcing mechanisms (Heeschen et al., 2005). Measurements of methane concentrations over time have shown a relation with tidal forces, albeit mostly in water less than 100 m deep (e.g. Mikolaj and Ampaya, 1973; Boles et al., 2001). Measurements with METS (Franatech GmbH) sensors over several days in deep water have been reported, with additional geochemical measurements, from seeps at Hydrate Ridge (Cascadia accretionary margin, offshore Oregon) by Bussell et al. (1999).

During New Vents cruise SO191 aboard RV SONNE, METS methane sensors were mounted on ocean bottom seismometers (OBS) and left for several days at seep sites deeper than 800 m off the southeastern tip of North Island, on the southern Hikurangi Margin (Fig. 1 inset, see Netzeband et al., this issue). Methane concentrations were measured

* Corresponding author. Tel.: +49 431 600 2418; fax: +49 431 600 2922.
E-mail addresses: akrabbenhoeft@ifm-geomar.de (A. Krabbenhoeft), Gesa.Netzeband@rwe.com (G.L. Netzeband), jbialas@ifm-geomar.de (J. Bialas), cpapenberg@ifm-geomar.de (C. Papenberg).
URL: http://www.rwedea.com (G.L. Netzeband).
[1] Now at RWE Dea AG, Überseering 40, D-22297 Hamburg, Germany.
[2] Tel.: +49 40 6375 2567; fax: +49 40 6375 3164.
[3] Tel.: +49 431 600 2329; fax: +49 431 600 2922.
[4] Tel.: +49 431 600 2330; fax: +49 431 600 2922.

0025-3227/$ – see front matter © 2009 Elsevier B.V. All rights reserved.
doi:10.1016/j.margeo.2009.08.001

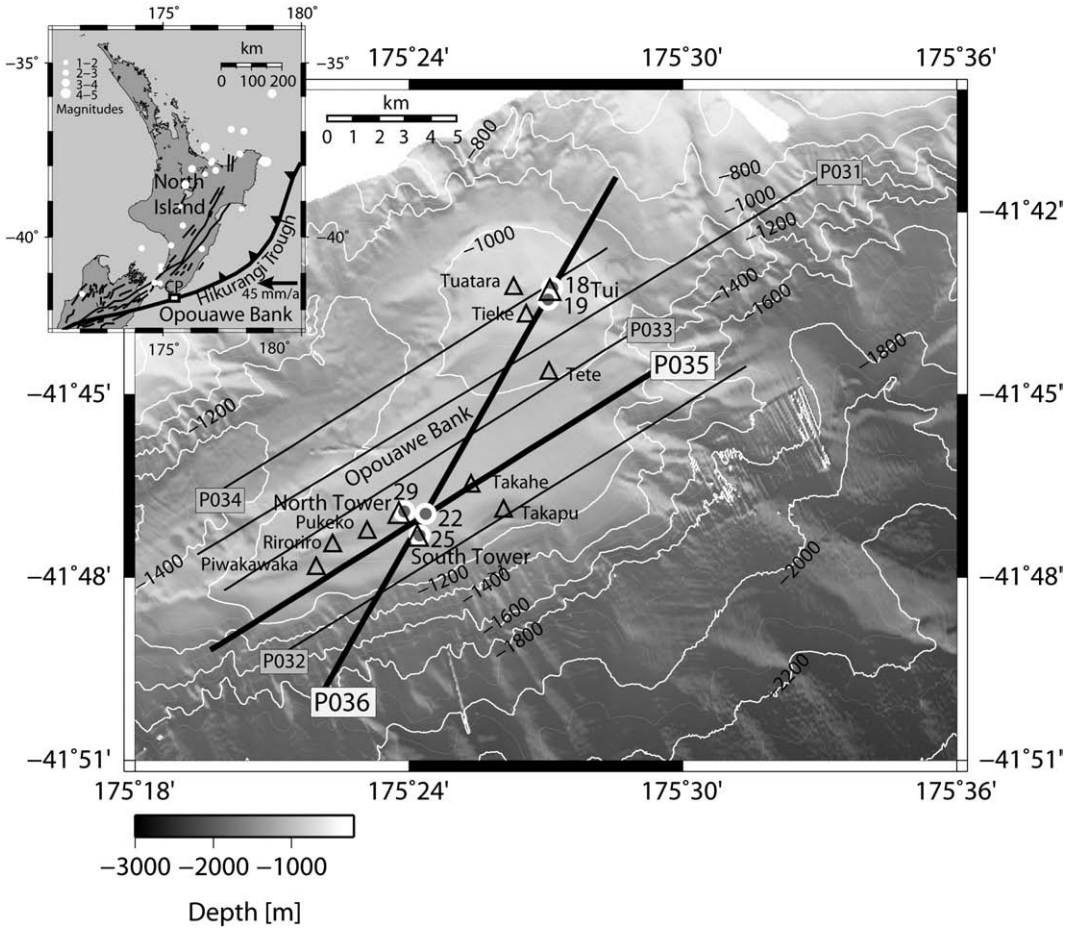

Fig. 1. Location of Opouawe Bank study area (inset) and sites of ocean bottom methane (OBM) sensors (grey-filled white circles) shown on grey-scale bathymetry with 100 m contours and depths in meters (bathymetry courtesy of Greinert et al., this issue). OBM18 and 19 are close to the Tui seep site at the elevated northeastern end of Opouawe Bank. OBM25 and 29 are close to the South Tower and North Tower seep sites on the southwest part of the ridge. OBM22 is distant from seep sites to monitor background conditions. Black lines indicate the seismic profiles; the bold lines, P035 and P036, are the profiles discussed in this paper. Known vent sites are marked by annotated triangles, the ones in the proximity of the ocean bottom methane stations are annotated in bold. White circles on the inset diagram show locations of earthquakes (magnitudes range from 1 to 5) recorded during the time that the OBMs were deployed (earthquake information from http://www.geonet.org.nz/. CP: Cape Palliser.

in-situ at fixed points a few centimetres above the seafloor for the duration of seismic surveys of the seep sites, typically for about two days. The aim was to record time series of methane concentrations at each location, and to compare different patterns of methane emission with seismic reflection images of the subseafloor structure. Locations for deploying the ocean bottom instruments carrying a methane sensor, hereafter called ocean bottom methane (OBM) stations, were chosen at known active vent sites (Fig. 1) based on previous acoustic investigations (Bialas et al., 2007).

1.1. Tectonic setting of OBM sites

A detailed description of the geological setting of the Hikurangi Margin including the area off the southeastern tip of North Island is given by Barnes et al. (this issue). Areas investigated with ocean bottom instrumentation, OBS and OBM, were Opouawe Bank in the South, Uruti Ridge in the middle, and Omakere Ridge (LM-9) in the North (Bialas et al., 2007). In this publication we concentrate on data from the Opouawe Bank area at the southern end at Hikurangi Margin. Opouawe Bank is a SW–NE trending ridge with a flat-topped elevated structure at its northeastern tip. The ridge is formed by imbricate-thrusting and dextral slip on the over-riding Indian Plate, just landward of an offscraped accretionary prism, as the Pacific Plate subducts obliquely beneath it (Barnes et al., this issue). Five OBMs were deployed in water depths ranging from ~800 m to ~1200 m (Fig. 1). They were located on seismic lines P035 and P036. The seismic survey, including multichannel seismic (MCS) data, is discussed in detail by Netzeband et al. (this issue).

Numerous vent sites are known at the Hikurangi Margin from previous studies (e.g. Lewis and Marshall, 1996; Greinert et al., this issue). Our OBM stations were clustered around known seep sites (Fig. 1). Additional seep sites were found during cruise SO191 using several methods, the ones mapped by sidescan sonar (Klaucke et al., this issue) are shown in Fig. 1; flare imaging in the water column (gas bubbles rising from the seafloor) showed Tui, North Tower, South Tower (the ones in the vicinity of our METS locations) Pukeko, and Takahe to be active.

OBM18 and OBM19 were placed on the elevated bank at the northeastern end of Opouawe Bank in the vicinity of the Tui vent site. Precise coordinates of Tui vent site were not known at the time of deployment, so the OBMs were deployed with reference to the bathymetric structure and were later found to be on each side of the seep. In the southwestern part of Opouawe Bank, OBM29 and OBM25 were placed near the North Tower and South Tower seeps, and OBM22 was placed ~1 km off the seep locations, to register a background methane signal where no active venting occurs at the crossing point of seismic profiles P035 and P036.

2. Methodology

Methane gas concentration dissolved in the water is detected by a METS (Franatech GmbH) sensor (e.g. Faure et al., 2006, Paull et al.,

Please cite this article as: Krabbenhoeft, A., et al., Episodic methane concentrations at seep sites on the upper slope Opouawe Bank, southern Hikurangi Margin, New Zealand, Mar. Geol. (2009), doi:10.1016/j.margeo.2009.08.001

2007). The sensor is based on the semi-conductor technology (e.g. Faure et al., 2006; Boulart, et al., 2008). Adsorption of hydrocarbons at the active layer of the semi-conductor leads to electron exchange with oxygen and thus to modification of the conductivity of the active layer. The conductivity is converted into voltage, which then is the output signal (U_{meth}). The methane signal is temperature dependent due to the semi-conductor technology. To separate real methane anomalies from sensor-specific temperature anomalies, another sensor output voltage signal is assigned to the temperature (U_{temp}). The operational values for the sensor are methane gas concentrations in the range of 50 nM to 10 μM and temperature in the range of −2 °C to +60 °C, which covers the typical range limits in seawater at active cold seeps. Calibration of the sensor is conducted at 100% humidity in fluids with different (known) methane gas concentrations and temperatures.

During the SO191-1 experiment, five methane sensors were deployed (Fig. 1). The logging interval during the acquisition time was set to 1 min. Each sensor was calibrated prior to deployment to determine sensor-specific conversion formulae expressing methane concentration and temperature in terms of voltage. Certain conditions, such as exposing the sensors to very high methane gas concentrations over long periods of time or extremely variable conditions of temperature, humidity, gas composition, or methane concentrations, can cause the sensor response to drift, requiring re-calibration. Although the sensors were operated and handled with care, we found a marginal drift in the sensor's response during the cruise. The effect of this was corrected by keeping the sensors in a seawater tub and comparing METS values with methane concentrations of the surface seawater measured with a gas chromatograph (GC) (Greinert, J., pers. Communication; for method description see Faure et al., this issue). After the cruise, methane concentrations from the GC were used as reference values for re-calibration of our METS data (Fig. 2). In this study we present the re-calibrated data. The methane and temperature voltages are shown in Fig. 2a. The calculated methane concentrations/temperatures before (Fig. 2b/d) and after re-calibration (Fig. 2c/e) for all sensors (solid lines) are shown with the reference methane/temperature values from the GC (dotted line). Here, the temperature dependence of the methane voltage signal is marked by dashed lines (Fig. 2a). After application of the conversion formulae the sensor temperature dependency is filtered in the methane signal (Fig. 2b, c). Differences of the METS temperatures compared to the GC temperature, for example between 18:00 and 21:00 UTC on the 27.01.2007 are attributed to the test arrangement, where the GC and METS thermometers measure the water temperature in different places. The sensor re-calibration using this method yields an error of 10% for absolute methane concentration values and temperatures. The general trend and orders of magnitude for methane concentrations at active and non-active seep sites observed with these time series are confirmed by comparing our METS data with measurements using CTD casts and different METS sensors in the water column in the same research area (Bialas et al., 2007; Faure et al., this issue).

3. Results

Data compiled from all sensors show small regional variations in the observed methane concentrations (Figs. 3 and 4). One data set of methane and temperature voltages, those of OBM18, is shown as an example (Fig. 3a). The calculated methane concentrations and temperatures are displayed in Fig. 3b and c for OBM18 and OBM19, respectively, both at the Tui site (Fig. 1). The calculated methane concentrations and temperatures for stations on the southwestern Opouawe Bank (OBM22, OBM25, and OBM29) are shown in Fig. 4. High and low tides, (obtained from the online service of the National Institute of Water & Atmospheric Research, New Zealand for nearby Cape Palliser (CP, inset Fig. 1), http://www.niwa.co.nz/our-services/online-services/tide-forcaster) are also displayed in Figs. 3 and 4 to allow correlation with our measured signals.

Methane concentrations from OBM18 and OBM19 show significant differences (Fig. 3b, c). The scale for the methane concentration reaches maximum values up to 14 μM at station OBM18, whereas the maximum values of the methane concentration for OBM19 only reach around 0.6 μM. The largest methane anomaly (labelled peak 5) recorded from OBM18, which lasted for ~4 h on Jan. 22nd, from around 14:00 to 18:00 UTC, has more than ten times larger values than any recorded at the other stations. It is preceded by two smaller peaks with methane concentration values up to 6 μM (peaks labelled 3 and 4) from around 9:00 to 13:00 UTC. After the prominent anomaly at peak 5, the remaining records show lower methane concentrations of <4 μM. The data from OBM18 show episodically high methane concentrations lasting for periods of several hours with higher frequency fluctuations around the temporarily elevated methane concentrations with periods of <1 h. On instrument OBM18 even the smaller anomalies with values up to ~3 μM are higher than the maximum values (1 μM) observed at the other OBM stations (Figs. 3c, 4). In contrast, the largest methane-concentration anomalies at OBM19 are single peaks with duration of roughly 30 min. They typically reach the maximum value rapidly (within a few minutes), and then decay more slowly to the background level <50 nM. The decay time is partly controlled by the sensor relaxation (slow diffusion of methane out of the sensor and the also slow oxidation processes of methane in the sensor), but is also tied to the intensity of the methane-concentration anomaly. Two examples are the methane anomalies of Jan. 22nd at 22:00 and Jan. 23rd at 01:00 UTC on instrument OBM 19 (peaks 6 and 7, Fig. 3c).

The methane concentrations of the southeastern cluster of OBM stations (OBM22, 25, and 29) range from 0 to 1 μM (Fig. 4). The most prominent anomaly is number 5 for “background level” station OBM22 (Fig. 4a), 11 for OBM25 (Fig. 4b), and 4 for station OBM29 (Fig. 4c). Anomaly 11 is large at OBM29 as well, but does not register at OBM22. At OBM22 (background) the first three methane peaks are very small (less than 50 nM above the background signal). After peak number 5, no further anomalies are registered at this station (Fig. 4a).

The temperature signals at each site show the same temporal behaviour, with similar patterns of amplitude with time (Figs. 3 and 4). They do not show clear correlations with methane concentrations. The temperatures range around 5 to 6 °C for the northwestern area, which are slightly higher than the ones for the southeastern region where values are around 4 °C (Figs. 3 and 4). The correlation with semi-diurnal tides is more striking at the northeastern (Fig. 3) than at the southwestern stations (Fig. 4).

Some results from other studies of cruise SO191, using different methodologies, are important for discussion of our results. Sidescan sonar mapping shows that the seep sites are about ~250 m in diameter, while active seep areas, where fluid escapes the seafloor, are only <50 m across (Klaucke et al., this issue); the larger extent of the seeps is below the seafloor, where bedding-parallel gas accumulation is inferred a few meters to a few tens of meters below the seafloor (bsf). Multiple flares in the water column observed at one seep area with the sidescan sonar (Klaucke et al., this issue) and by ROV dives (Naudts et al., this issue) reveal that seep areas consist of several active vents (Bialas et al., 2007). These are temporally variable, i.e. some being active/inactive, when revisited (Klaucke et al., this issue). Faure et al. (this issue) found methane concentrations of ~920 nM close to the seafloor near Tui seep site and ~120 nM 50 m above the seafloor (~1000 m below sea level) near North Tower. These values are smaller than the values observed with our METS (around 1000 nM–4000 nM, with maximum values ~14 μM at Tui site and elevated methane values in the range of 100 nM up to 700 nM around North Tower), which is reasonable because we measured directly at the seafloor and most likely closer to the seep. Faure et al. (this issue)

Please cite this article as: Krabbenhoeft, A., et al., Episodic methane concentrations at seep sites on the upper slope Opouawe Bank, southern Hikurangi Margin, New Zealand, Mar. Geol. (2009), doi:10.1016/j.margeo.2009.08.001

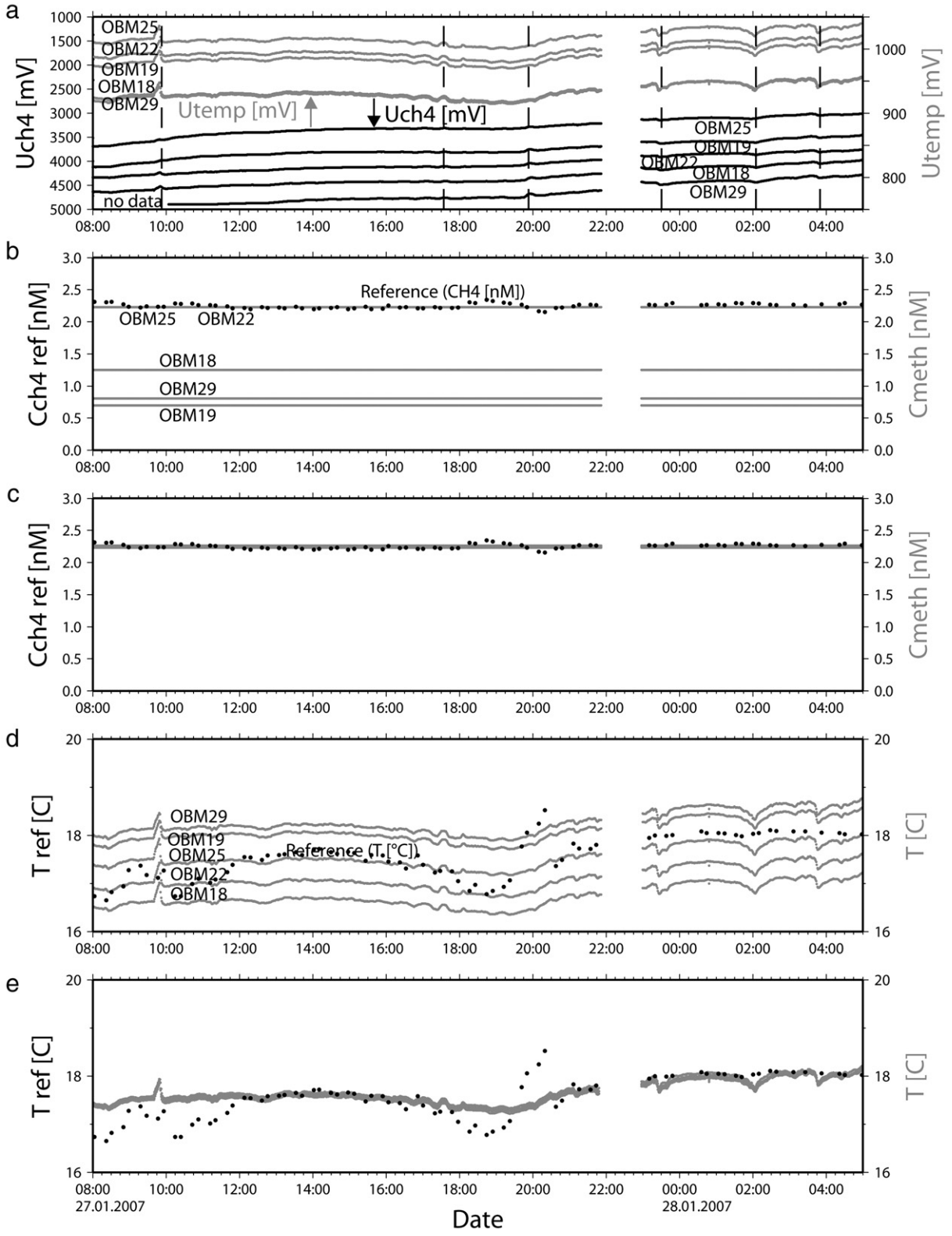

Fig. 2. Calibration of methane sensors in a surface seawater tub. Panel (a) shows the methane (black) and temperature (grey) voltage output. Panel (b) shows methane concentrations relative to a reference methane concentration from gas chromatography (GC) (black dots). Panel (c) shows the re-calculated methane concentration for all OBM sensors together with the methane reference (black dots). Panel (d) shows calibrated temperature values for the 5 sensors relative to the reference temperature (black dots). Panel (e) shows the re-calculated temperatures relative to the temperature reference (black dots).

found the prevailing water current direction to be southward and Klaucke et al. (this issue) determined bottom water currents to range from southward to south-westward, deduced from deflection of the rising flares. Adjacent active seeps show different gas escape frequency and seepage activity rates; sometimes gas escape occurs at neighbouring sites simultaneously, at other times gas discharge is alternating, and fluid flow intensity can vary between periods of non-activity and violent outbursts (Naudts et al., this issue).

Please cite this article as: Krabbenhoeft, A., et al., Episodic methane concentrations at seep sites on the upper slope Opouawe Bank, southern Hikurangi Margin, New Zealand, Mar. Geol. (2009), doi:10.1016/j.margeo.2009.08.001

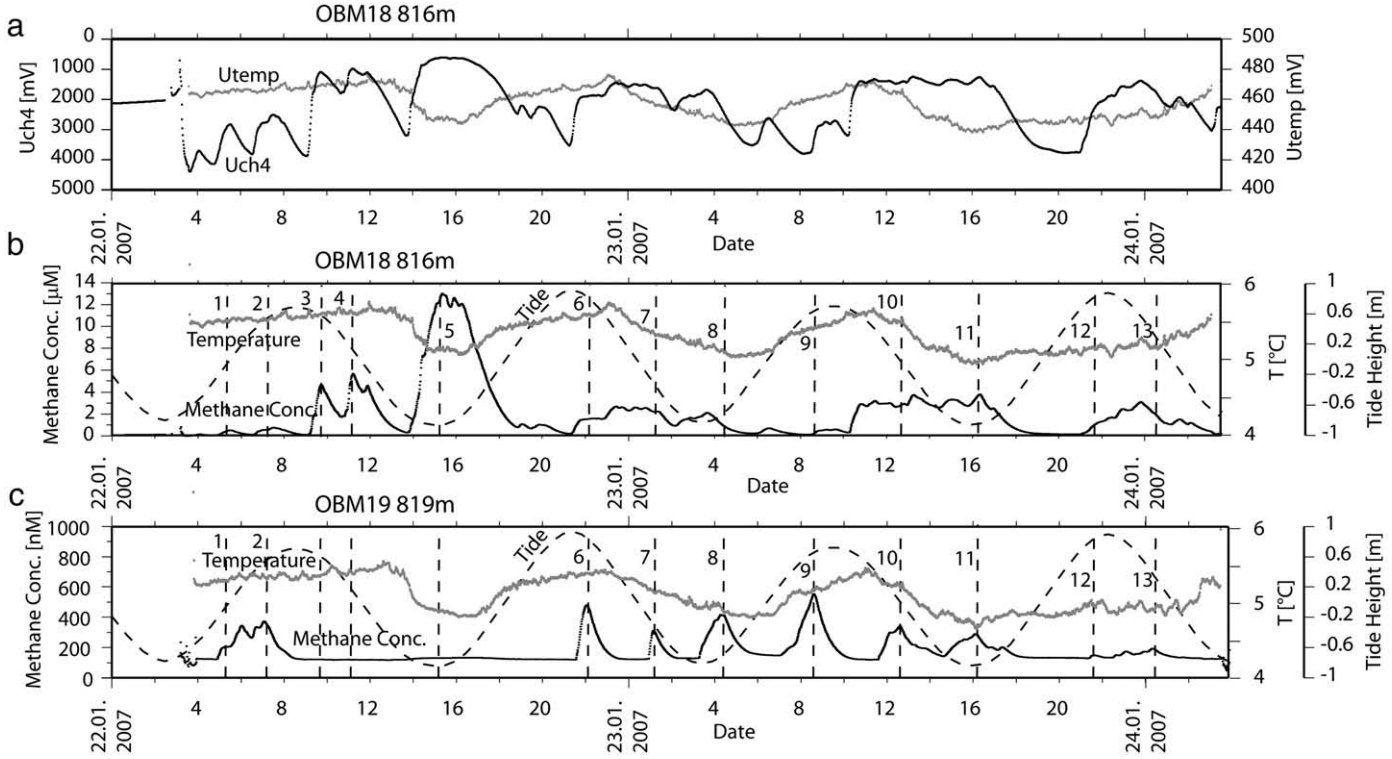

Fig. 3. Methane concentrations, temperature and tidal height against time at the Tui site. (a) Voltage outputs of sensor OBM18, methane (Uch4, black) and temperature voltages (U_{temp}, grey) are measured in mV. (b and c) The methane concentration in µM for OBM18 and in nM for OBM19 (black) and temperature in °C (grey) calculated from the voltages. Peaks in methane concentration are numbered. Tides are plotted as dashed line.

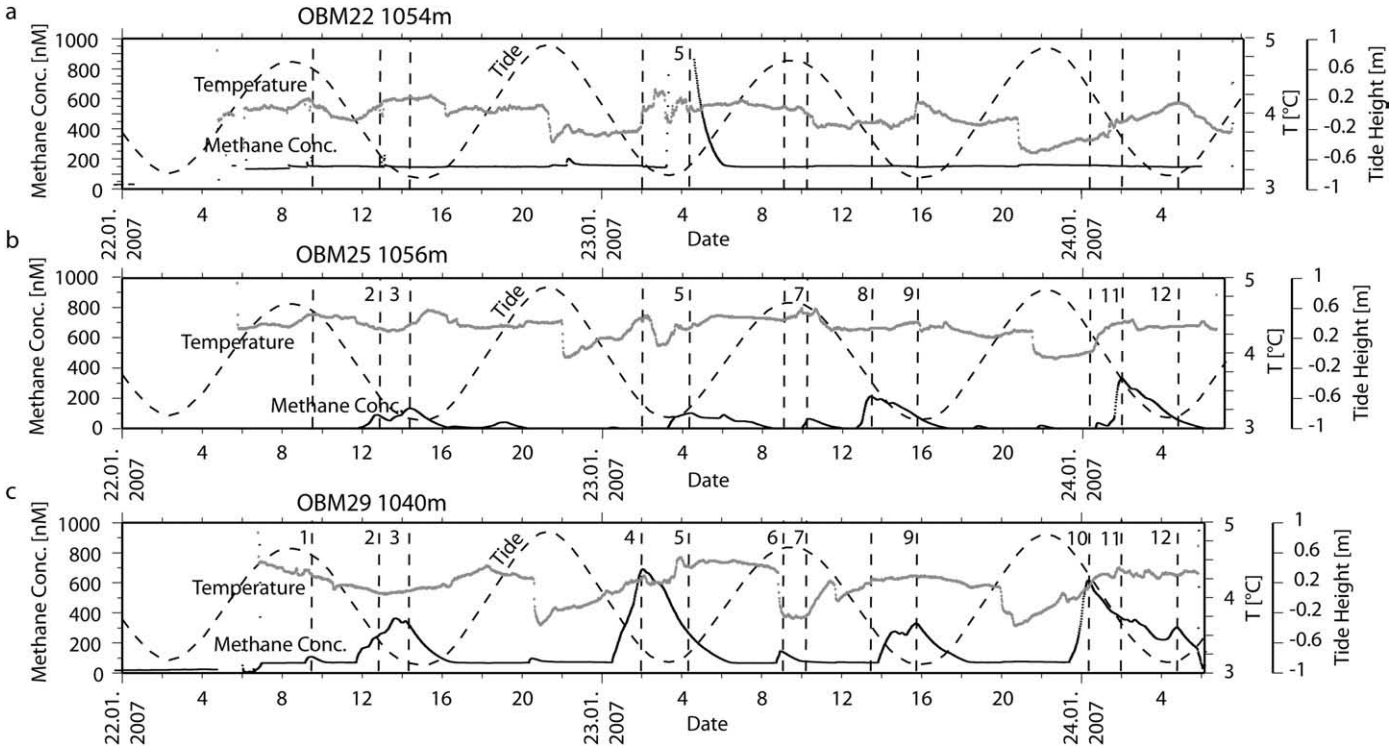

Fig. 4. Methane concentrations, temperature and tidal height against time at the southwestern seep sites near the crossing point of seismic profiles P035 and P036 for (a) station OBM22, (b) OBM25, and (c) OBM29. Methane concentration is given in nM and temperature in °C. Prominent features are numbered. Tides are plotted as dashed line.

4. Discussion

In general, seep structures as observed in the study area (Lewis and Marshall, 1996; Faure, et al., 2006) can be pathways for overpressured pore fluids generated by sediment compaction or pathways for free gas, i.e. methane and higher hydrocarbons (e.g. Minshull and White, 1989). Also, BSRs indicative of natural gas hydrates, are closely linked to gas seepage at the seafloor in this area (e.g. Pecher et al., this issue). In the following, we discuss the relation of our methane concentration measurements with underlying

Please cite this article as: Krabbenhoeft, A., et al., Episodic methane concentrations at seep sites on the upper slope Opouawe Bank, southern Hikurangi Margin, New Zealand, Mar. Geol. (2009), doi:10.1016/j.margeo.2009.08.001

geological structures and with natural events, such as earthquakes and tidal forces. Several seismic structures associated with fluid venting at Opouawe Bank are discussed in detail by Netzeband et al. (this issue). Therefore we focus on the structures that are related to the observed methane expulsion at the OBM deployment locations. The relationship between seismic characteristics as interpreted by Netzeband et al. (this issue) and the distribution of OBM stations along P035 and P036 are shown in Figs. 5 and 6. Other possible fluid migration pathways ("seeps") are indicated as well as zones with bedding-parallel gas fronts (ellipses) a few meters below the OBM sites (Figs. 5 and 6).

The differences in methane concentrations measured at the different stations could principally relate to their locations relative to active vents. OBM18 and OBM19 were placed on top of a bathymetric high in a water depth of ~820 m; Tui seep site is located within perhaps a few tens of meters of these instruments. OBM22, OBM25, and OBM29 were placed on a filled slope basin near the crest of the SW–NE trending ridge in water depths of ~1050 m close to the North Tower and South Tower seep sites.

The deployment of the ocean bottom instruments was not video guided, but the significantly higher (one order of magnitude) methane concentrations at OBM18, up to 14 μM compared with maximum values of ~1 μM at the other stations, suggest that OBM18 is likely to be located within a few meters of, if not right at, a vent at Tui seep site (Figs. 1, 2, and 3). We speculate that the observed high methane bursts at OBM18 represent fluid outbursts at the Tui seep.

The structure beneath OBM18 shows disturbance of the seismic reflections in the MCS data (Fig. 6), probably caused by fracturing and high permeability of the sediments indicative of upward movement of fluids (e.g. Pecher et al., 2004). Near the seabed, the conduit is covered by a layer of undisturbed sediment. But looking closely, a small fault structure in the uppermost sedimentary layer can be identified underneath OBM18 in high resolution subbottom profiles (Klaucke et al., this issue). The fluid conduit is connected with the seafloor by a fault that is feeding the area of elevated methane expulsion observed at OBM18. Thus, this conduit almost certainly feeds the Tui seep site. The conduit reaches downwards to a depth of at least 0.5 s TWT bsf, which is the depth of the bottom simulating reflector (BSR) (see Netzeband et al., this issue). Geochemical analysis indicates that the methane gas venting is of biogenic origin (Faure et al., this issue). The gas might be captured and transported upwards with rising fluids from the dewatering sediments at the top of the subducting oceanic crust (Townend, 1997) and within sediments of the upper plate (Lewis and Marshall, 1996). At Opouawe Bank, the limited continuity of the BSR, and hence the hydrate seal, might be evidence for large fluid flow indicated by the large and long-lasting methane anomalies

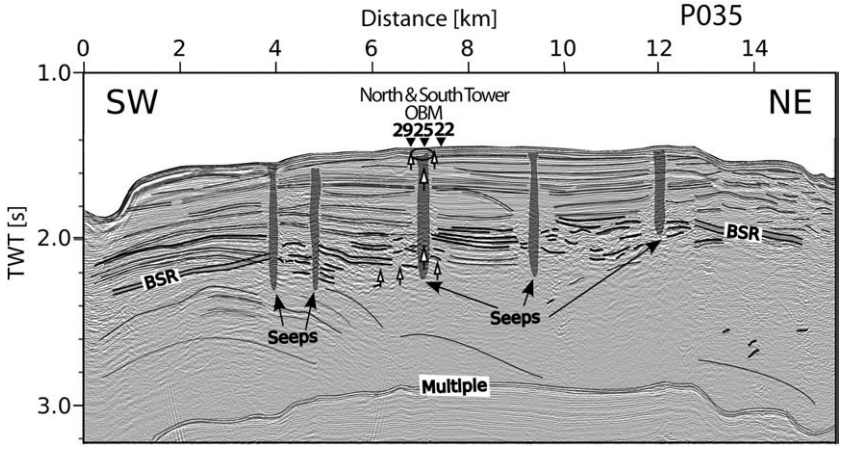

Fig. 5. Line interpretation on MCS line P035 with positions of OBM sites 22, 25 and 29 indicated by black triangles. OBM25 and 29 are offline and projected onto the profile. The grey shaded columns indicate diffuse bedding interpreted to be a result of fluid seepage. The BSR, where observed, is marked by a filled double line. Inferred fluid flow is indicated by white filled arrows. Circle indicates where bedding-parallel gas accumulates.
(profile modified from Netzeband et al., this issue).

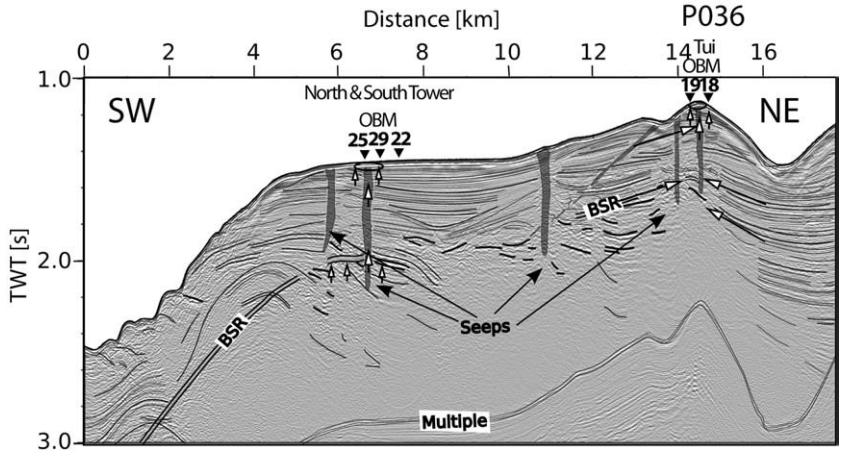

Fig. 6. Line interpretation on MCS line P036 with positions of all OBM sites indicated by black triangles. OBM29 is offline and projected onto the profile. The grey shaded columns indicate diffuse bedding interpreted as resulting from fluid seepage. The BSR, where observed, is marked by a filled double line. Fluid flow is indicated by white filled arrows. Circle indicates where bedding-parallel gas accumulates. Note the slant chimney/fault plane terminating at the seafloor at km 14.
(profile modified from Netzeband et al., this issue).

Please cite this article as: Krabbenhoeft, A., et al., Episodic methane concentrations at seep sites on the upper slope Opouawe Bank, southern Hikurangi Margin, New Zealand, Mar. Geol. (2009), doi:10.1016/j.margeo.2009.08.001

at OBM18 and a geochemical plume of high methane concentrations in the water column despite the strong tidal currents in the bottom waters (see Faure et al., this issue).

The methane concentration anomalies observed at OBM19 have much smaller values than the ones observed on OBM18. This may indicate increased distance from a seep or a more diffuse subbottom supply close to the OBM19 site.

Several gas conduits similar to that at the Tui site, some of them covered by sedimentary layers, are observed in seismic sections P035 and P036, and also beneath OBM25 and OBM29 (Figs. 5 and 6). However, at the southwestern North Tower and South Tower sites, in the vicinity of OBM25 and OBM29, we measured significantly smaller methane concentrations than at OBM18. In both areas, beneath OBM18 and OBM19, as well as beneath OBM22, OBM25, and OBM29, columns of diffuse seismic reflectivity indicate fluid conduits that extend upwards to within a few meters of the seabed. The subbottom profiler (Klaucke et al., this issue) shows these conduits covered by thin layers of undisturbed sediment.

Another explanation for the differences of fluid flow patterns and expulsion rates between the northeastern and southwestern seep sites might relate to their structural setting. OBM22, OBM25, and OBM29 are located above a sedimentary basin with well stratified sedimentary layers up to about 700 m thick. Slope basin sediments are typically muddy (Lewis, 1973; Lewis and Kohn, 1973) and probably have low permeability. Here, vertical fluid flow is expected to be slow and may occur in transient events probably due to sediment compaction (e.g. Sahling, et al., 2008). The conduits we see in the slope basin underneath OBM stations 22, 25, and 29 appear to be sealed at the seafloor with undisturbed sedimentary layers (Figs. 5 and 6). One might speculate that they represent paleo-conduits, but more likely they are still active with diffuse as well as direct connections to the seafloor along small faults outside the plain of the seismic section. Flares occurred at North Tower along sidescan profile P035 as well as South Tower along P036. OBM29 and OBM25 are inferred to be located within a few tens of meters of the North Tower and South Tower sites, respectively. We suggest that there may also be diffuse gas emission through the well stratified sedimentary layers of the slope basin. We interpret this gas distribution to be wider in lateral extent, which is supported by the stronger and wider distribution of the BSR compared with Tui seep site. This may explain the lower fluid flow rates at the southeastern sites compared to the higher methane anomalies in the northeast, where the subsurface structure and the elevated seafloor may focus gas accumulation leading to high flow rates.

Another possible explanation for the differences in methane concentrations might be the bottom water currents. As stated before, we believe, that OBM18 is located very close to or directly above an active seep. The smaller methane concentrations at OBM19, OBM25, and OBM29 and their southern or southwestern locations relative to the active seeps Tui, South Tower, and North Tower, respectively, might suggest that bottom water currents moving southwards or southwestwards as observed by Faure et al. (this issue) and Klaucke et al. (this issue) are likely to distribute the methane from seep locations towards the METS stations; this might lead to the elevated methane concentrations observed at these stations, with values much lower than those recorded virtually right at a seep site such as is inferred for OBM18. Arguing against this hypothesis, that elevated methane concentrations observed at OBM19, OBM25, and OBM29 are current-distributed seep signals, are the methane anomalies observed at OBM22 despite its upstream location of all known active seep sites. Also, bubbles and dissolved methane rise well above the seabed (Faure et al., this issue) and may have limited effect on the seabed nearby as dissolution and distribution mainly happens in the water column a few to tens of meters above the bottom. These observations suggest a stronger influence of sedimentary processes on enhanced fluid flow rather than currents being the primary influence on METS registrations.

The temperatures at OBM18 and OBM19 are around 5–6 °C, a degree or two higher than the 4–5 °C at OBM22, 25, and 29. This may partly relate to the difference in water depth of ~820 m compared with ~1050 m (compare CTD measurements of Faure et al., this issue). The slightly higher temperature signal of ~0.3 °C at OBM18 compared with OBM19 might originate from the warm fluids that escape the seafloor there, as recorded by the high methane concentrations at OBM18 compared with OBM19. The same might apply for OBM22, 25, and 29, where the temperature of OBM22 is ~0.5 °C less than the two stations close to the seep sites. However, it must be noted, that temperature differences are within the error range (10%) of the sensors. Temperature signals from all stations correlate principally with the tidal signal.

The methane signals also show some tidal dependency. It has been suggested that enhanced fluid flow may occur during high tides due to higher fluid overpressure (e.g. Judd and Hovland, 2007, and references therein), although elevated fluid flows have also been observed during low tides (e.g. Boles et al., 2001; Torres et al., 2002). At Opouawe Bank, all stations show some increases in methane seepage at low tides. As proposed by Boles et al. (2001), Torres et al. (2002), and also shown by Linke et al. (this issue), fluid discharge at the seafloor might be facilitated by the lower hydrostatic pressure during low tide. The deeper stations in the southwest (OBM22, 25, and 29) show stronger dependence on the semi-diurnal tidal forcing than the shallower ones in the northeast (OBM18 and 19). Because the southwestern sites were located above horizontally layered sediments, we argue that the tidal changes of pressure have a stronger influence than at OBM18 and 19, which are situated at an anticline where fluid flow is more focused and less affected by reduced hydrostatic pressure during low tide.

Studies of other active margins have shown that high methane concentrations in the seawater and increased fluid venting are closely related to moderate and strong earthquakes (Obzhirov et al., 2004; Brown et al., 2005). In some areas, seep activity serves as a precursor for earthquakes (Huang et al., 1998). Although several small to moderate earthquakes (magnitudes range from 1 to 5) occurred beneath North Island during the period of OBM deployment (Fig. 1, inset, earthquake information from http://www.geonet.org.nz/), none were close to the deployment and no convincing correlation with gas anomalies can be found.

We speculate that structural and sedimentary mechanisms are the main influence on the observed variability in methane concentrations recorded with the METS at Opouawe Bank. Reduced hydrostatic pressure enhanced the elevated methane concentrations during low tides. Additionally bottom water currents may also play a secondary role in elevating methane concentrations.

5. Conclusion

On Opouawe Bank numerous events of episodic gas flow detected with methane and temperature sensors (METS) show a high variability in space and time. Elevated fluid flows, lasting a few minutes to several hours alternate with periods of quiescence also varying from several minutes to several hours. Different patterns of enhanced methane expulsion are observed. We infer that the differences are generally related to different fluid flow mechanisms in the underlying sediment structure, with more diffuse fluid flow at the southwestern North Tower and South Tower sites above basin sediments, and more focused fluid flow at the northeastern Tui vent site on a structural high.

At active vent sites, the maximum methane concentration is as high as 14 μM. In the northeast at Tui site, small faults cutting through the uppermost layers may assist near vertical and focused fluid migration resulting in high methane concentrations. In contrast, at the southwestern North Tower and South Tower sites, methane discharge is moderate to low, with typical maximum values of up to 1 μM above

Please cite this article as: Krabbenhoeft, A., et al., Episodic methane concentrations at seep sites on the upper slope Opouawe Bank, southern Hikurangi Margin, New Zealand, Mar. Geol. (2009), doi:10.1016/j.margeo.2009.08.001

thick slope basin sediments, where a widely distributed BSR suggests widely distributed gas. There, discharge of fluids at the seafloor is speculated to occur through smaller fluid pathways in the planar bedding, compared with the focused discharge at Tui seep. It is inferred that reduced hydrostatic pressure during low tides promotes episodic methane seepage, predominantly at the southwestern North Tower and South Tower sites. The semi-diurnal signal of the tides is also evident in the temperature recordings and there are slightly elevated temperatures at the sites closest to active vents, although these are within the probable error range of the sensors. The strong tidal currents contribute to the quick dilution of methane gas in the surrounding seawater but it inferred that they have a relatively minor influence on fluctuating methane concentrations, which are considered to be the result of transient local discharge events. There is no link between elevated methane discharge from the seafloor and earthquake occurrences during the experiment.

Acknowledgements

We would like to thank the captain, crew and scientific staff of cruise SO191-1 onboard RV SONNE, for their excellent support. Discussion with E. Suess on general issues concerning the METS ahead of writing the draft, helped clarify uncertainties. Most of the figures were made with the Generic Mapping Tool (GMT) free software (Wessel and Smith, 1998). We wish to thank the associated editors, K. Lewis and J. Greinert, and two unknown reviewers for their discussion and careful and constructive reviews, who helped improve an earlier version of the manuscript. The New Vents project was funded by the German Ministry of Education and Research (BMBF) grant no. 03G0191A.

References

Barnes, P.M., Lamarche, G., Bialas, J., Henrys, S., Pecher, I., Netzeband, G.L., Greinert, J., Mountjoy, J.J., Pedley, K., and Crutchley, G., 2009. Tectonic and geological framework for gas hydrates and cold seeps on the Hikurangi subduction margin, New Zealand. Mar. Geol. doi:10.1016/j.margeo.2009.03.012.

Berndt, C., 2005. Focused fluid flow in passive continental margins. Phil. Trans. R. Soc. A 363, 2855–2871.

Bialas, J., Greinert, J., Linke, P., Pfannkuche, O., 2007. FS SONNE cruise report SO191 New Vents—"Puaretanga Hou". IFM-GEOMAR Report 9 190 pp., ISSN: 1614-6298.

Bohrmann, G., Ivanov, M., Foucher, J.-P., Spiess, V., Bialas, J., Greinert, J., Weinrebe, W., Abegg, F., Aloisi, G., Artemov, Y., et al., 2003. Mud volcanoes and gas hydrates in the Black Sea: new data from Dvurechenskii and Odessa mud volcanoes. Geo-Mar. Lett. 23, 239–249.

Boles, J.R., Clark, J.F., Leifer, I., Washburn, L., 2001. Temporal variation in natural methane seep rate due to tides, Coal Oil Point area, California. J. Geophys. Res. 106 (C11), 27077–27086.

Boulart, C., Mowlem, M.C., Connelly, D.P., Dutasta, J.-P., German, C.R., 2008. A novel, low-cost, high performance dissolved methane sensor for aqueous environments. Opt. Express 16 (17).

Brown, K.M., Tryon, M.D., DeShon, H.R., Dorman, L.M., Schwartz, S.Y., 2005. Correlated transient fluid pulsing and seismic tremor in the Costa Rica subduction zone. Earth Planet. Sci. Lett. 238, 189–203.

Bussell, J., Klinkhammer, G., Collier, R.W., Linke, P., Appel, K., Heeschen, K., Suess, E., De Angelis, M.A., Masson, M., Marx, S., 1999. Applications of the METS methane sensor to the in situ determination of methane over a range of timescales. EOS Trans. Am. Geophys. Union.

Faure, K., Greinert, J., Pecher, I.A., Graham, I.J., Massoth, G.J., de Ronde, C.E.J., Wright, I.C., Baker, E.T., Olsen, E.J., 2006. Methane seepage and its relation to slumping and gas hydrate at the Hikurangi Margin, New Zealand. N.Z. J. Geol. Geophys. 49, 503–516 0028-8306/06/4904-0503.

Faure, K., Greinert, J., Schneider V.D.J., McGinnis, D.F., Kipfer, R., Linke, P., 2009. Free and dissolved methane in the water column and the sea surface: Geochemical and hydroacoustic evidence of bubble transport. Mar. Geol.

Greinert, J., Lewis, K., Bialas, J., Pecher, I., Rowden, A., Linke, P., De Batist, M., Bowden, D., and Suess, E. Methane seepage along the Hikurangi Margin, New Zealand: Review of studies in 2006 and 2007. Mar. Geol., this issue.

Heeschen, K.U., Collier, R.W., de Angelis, M.A., Suess, E., Rehder, G., Linke, P., Klinkhammer, G.P., 2005. Methane sources, distributions, and fluxes from cold vent sites at Hydrate Ridge, Cascadia Margin. Glob. Biogeochem. Cycles 19 (2). doi:10.1029/2004GB002266.

http://www.geonet.org.nz/, New Zealand earthquake information.

http://www.niwa.co.nz/our-services/online-services/tide-forcaster, New Zealand tide information.

Huang, F., Zhang, X., Xia, X., Qiang, Z., Lin, C., Zhang, Y., 1998. Distribution of methane and its homologues in low-layer atmosphere over eastern China and seas. Chin. Sci. Bull 43 (22).

Judd, A., Hovland, M., 2007. Seabed Fluid Flow: The Impact on Geology, Biology, and the Marine Environment. Cambridge University Press. ISBN 9780521819503.

Klaucke, I., Weinrebe, W., Petersen, C.J., Bowden, D., 2009. Temporal variability of gas seeps offshore New Zealand: multi-frequency geoacoustic imaging of the Wairarapa area, Hikurangi margin. Mar. Geol. doi:10.1016/j.margeo.2009.02.009.

Kvenvolden, K.A., 1988. Methane hydrate—a major reservoir of carbon in the shallow geosphere? Chem. Geol. 71 (1–3), 41–51.

Kvenvolden, K.A., 1993. Gas hydrates—geologic perspective and global change. Rev. Geophys. 31, 173–187.

Kvenvolden, K.A., 1998. A primer on the geological occurrence of gas hydrate. In: Henriet, J.-P., Mienert, J. (Eds.), Gas Hydrates: Relevance to World Margin Stability and Climate Change: Geological Society, pp. 9–30.

Lewis, K.B., 1973. Sediments on the continental shelf and slope between Napier and Castlepoint, New Zealand. N.Z. J. Mar. Freshw. Res. 7, 183–208.

Lewis, K.B., Kohn, B.P., 1973. Ashes, turbidites, and rates of sedimentation on the continental slope off Hawkes Bay. N.Z. J. Geol. Geophys. 16, 439–454.

Lewis, K.B., Marshall, B.A., 1996. Seep faunas and other indicators of methane-rich dewatering on New Zealand convergent margins. N.Z. J. Geol. Geophys. 39, 181–200.

Linke, P., Sommer, S., Rovelli, L., McGinnis, D.F., 2009. Physical limitations of dissolved methane fluxes: The role of bottom-boundary layer processes. Mar. Geol. doi:10.1016/j.margeo.2009.03.020.

Mau, S., Rehder, G., Arroyo, I.G., Gossler, J., Suess, E., 2007. Indications of a link between seismotectonics and CH4 release from seeps off Costa Rica. Geochem. Geophys. Geosyst. 8, Q04003. doi:10.1029/2006GC001326.

Mikolaj, P.G., Ampaya, J.P., 1973. Tidal effects on the activity of natural submarine oil seeps. Mar. Technol. Soc. J. 7, 25–28.

Milkov, A.V., 2005. Molecular and stable isotope compositions of natural gas hydrates: a revised global dataset and basic interpretations in the context of geological settings. Org. Geochem. 36 (5), 681–702.

Minshull, T., White, R., 1989. Sediment compaction and fluid migration in the Makran accretionary prism. J. Geophys. Res. 94 (B6), 7387–7402.

Naudts, L., Greinert, J., Poort, J., Belza, J., Vangampelaere, E., Boone, D., Linke, P., Henriet, J.-P., and De Batist, M., 2009. Active venting sites on the gas-hydrate-bearing Hikurangi Margin, Off New Zealand: Diffusive-versus bubble-released methane. Mar. Geol. doi:10.1016/j.margeo.2009.08.002.

Netzeband G.L., Krabbenhoeft, A., Zillmer, M., Petersen, C.J., Papenberg, C., Bialas, J., 2009. The structures beneath submarine methane seeps: Seismic evidence from Opouawe Bank, Hikurangi Margin, New Zealand. Mar. Geol. doi:10.1016/j.margeo.2009.07.005.

Obzhirov, A., Shakirov, R., Salyuk, A., Suess, E., Biebow, N., Salomatin, A., 2004. Relation between methane venting, geological structure and seismo-tectonics in the Okhotsk Sea. Geo. Mar. Lett. 24, 135–139.

Paull, C., William Ussler III, W., Peltzer, E.T., Brewer, P.G., Keaten, R., Mitts, P.J., Nealon, J.W., Greinert, J., Herguera, J.-C., Perez, M.E., 2007. Authigenic carbon entombed in methane-soaked sediments from the northeastern transform margin of the Guaymas Basin, Gulf of California. Deep-Sea Res. II 54, 1240–1267.

Pecher, I.A., Henrys, S.A., Zhu, H., 2004. Seismic images of gas conduits beneath vents and gas hydrates on Ritchie Ridge, Hikurangi Margin, New Zealand. N.Z. J. Geol. Geophys. 47, 275–279.

Pecher, I.A., Henrys, S.A., Wood, W.T., Kukowski, N., Crutchley, G.J., Fohrmann, M., Kilner, J., Senger, K., Gorman, A.R., Coffin, R.B., Greinert, J., and Faure, K., 2009. Focused fluid flow on the Hikurangi margin, New Zealand—evidence from possible local upwarping of the base of gas hydrate stability. Mar. Geol.

Sahling, H., Bohrmann, G., Spiess, V., Bialas, J., Breitzke, M., Ivanov, M., Kasten, S., Krastel, S., Schneider, R., 2008. Pockmarks in the Northern Congo Fan area, SW Africa: complex seafloor features shaped by fluid flow. Mar. Geol. doi:10.1016/j.margeo.2007.11.010.

Suess, E., Torres, M.E., Bohrmann, G., Collier, R.W., Greinert, J., Linke, P., Rehder, G., Trehu, A., Wallmann, K., Winckler, G., et al., 1999. Gas hydrate destabilization: enhanced dewatering, benthic material turnover and large methane plumes at the Cascadia convergent margin. Earth Planet. Sci. Lett. 170 (1–2), 1–15.

Townend, J., 1997. Subducting a sponge: minimum estimates of the fluid budget of the Hikurangi margin accretionary prism. Geol. Soc. N.Z. Newslett. 112, 14–16.

Wessel, P., Smith, W.H.F., 1998. New, improved version of the Generic Mapping Tools released. EOS Trans. AGU 79, 579.

Please cite this article as: Krabbenhoeft, A., et al., Episodic methane concentrations at seep sites on the upper slope Opouawe Bank, southern Hikurangi Margin, New Zealand, Mar. Geol. (2009), doi:10.1016/j.margeo.2009.08.001